Physics and Astronomy

College of Arts and Sciences

2001

Heating and Ionization of the Intergalactic Medium by an Early X-Ray Background

Aparna Venkatesan
University of San Francisco, avenkatesan@usfca.edu

Mark L. Giroux

J Shull

Recommended Citation

HEATING AND IONIZATION OF THE INTERGALACTIC MEDIUM BY AN EARLY X-RAY BACKGROUND

APARNA VENKATESAN, MARK L. GIROUX,[1] AND J. MICHAEL SHULL

Center for Astrophysics and Space Astronomy, Department of Astrophysical and Planetary Sciences, University of Colorado, 389 UCB, Boulder, CO 80309-0389; aparna@casa.colorado.edu, giroux@casa.colorado.edu, mshull@casa.colorado.edu

ABSTRACT

Observational studies indicate that the intergalactic medium (IGM) is highly ionized up to redshifts just over 6. A number of models have been developed to describe the process of reionization and the effects of the ionizing photons from the first luminous objects. In this paper we study the impact of an X-ray background, such as high-energy photons from early quasars, on the temperature and ionization of the IGM prior to reionization, before the fully ionized bubbles associated with individual sources have overlapped. X-rays have large mean free paths relative to EUV photons, and their photoelectrons can have significant effects on the thermal and ionization balance. We find that hydrogen ionization is dominated by the X-ray photoionization of neutral helium and the resulting secondary electrons. Thus, the IGM may have been warm and weakly ionized prior to full reionization. We examine several related consequences, including the filtering of the baryonic Jeans mass scale, signatures in the cosmic microwave background, and the H^--catalyzed production of molecular hydrogen.

Subject headings: cosmology: theory — diffuse radiation — intergalactic medium — quasars: general — X-rays: general

1. INTRODUCTION

Observations of the spectra of high-redshift quasars and galaxies shortward of Lyα have revealed that the intergalactic medium (IGM) is highly ionized up to redshifts $z \sim 6$ (Fan et al. 2000; Hu, McMahon, & Cowie 1999; Spinrad et al. 1998). The reionization of the IGM subsequent to recombination at $z \sim 1000$ is thought to have been caused by increasing numbers of the first luminous sources, such as stars (Haiman & Loeb 1997; Fukugita & Kawasaki 1994), quasars (Donahue & Shull 1987; Valageas & Silk 1999), protogalaxies (Giroux & Shapiro 1996; Madau, Haardt, & Rees 1999; Ciardi et al. 2000; Chiu & Ostriker 2000; Gnedin 2000), or combinations of these (Giroux & Shapiro 1996; Tegmark, Silk, & Blanchard 1994).

It is unclear whether the H I and He II reionization epochs were coeval; it is certainly possible with a sufficiently hard ionizing source spectrum, from, e.g., quasars or zero-metallicity stars (Giroux & Shapiro 1996; Tumlinson & Shull 2000). The present data, however, indicate that He II reionization occurred at $z \sim 3$ (Jakobsen et al. 1994; Hogan, Anderson, & Rugers 1997; Reimers et al. 1997; Kriss et al. 2001), and that of hydrogen before $z \sim 6$. The degree to which QSOs influence the process of reionization depends on their relative abundance at high redshifts. There have been indications that the QSO space density decreases beyond a peak at $z \sim 3$. This has recently been corroborated by the Sloan Digital Sky Survey (SDSS) observations of high-z QSOs (Fan et al. 2001a, 2001b). However, QSOs may still be relevant to reionization, if they are powered by massive black holes that are postulated to form as a fixed universal fraction of the mass of collapsing halos at all redshifts (see, e.g., Magorrian et al. 1998; Kormendy & Gebhardt 2001), leading to a large population of miniquasars at

$z \gtrsim 6$ (Haiman & Loeb 1998). The observed turnover in the QSO space density at $z \gtrsim 3$ would then be true only for the brightest QSOs.

It is also possible that some high-z QSOs have been missed owing to dust obscuration. The most plausible scenario rests on evidence that the X-ray background (XRB) includes a substantial contribution from strongly absorbed active galactic nuclei (AGNs) with hard X-ray spectra (Gilli, Risaliti, & Salvati 1999). Recent results from the *Chandra* satellite (Mushotzky et al. 2000; Giacconi et al. 2001) also suggest that many of the resolved hard X-ray sources in the background could be AGNs in dust-enshrouded galaxies or a population of quasars at extremely high redshift. A contrary view is provided by Shaver et al. (1999), who used a sample of 442 radio-loud quasars, unhindered by dust selection effects, to confirm the rapid decline in quasar space density at $z > 2.5$.

In this paper we study the effects of an XRB, including the case of X-ray photons generated by high-z quasars, on the temperature and ionization of the IGM prior to full reionization. X-rays have much larger mean free paths than extreme ultraviolet (EUV) photons with energies ≥ 13.6 eV and can permeate the IGM relatively uniformly. Thus, they are capable of significantly heating the IGM prior to the epoch when the bubbles that are highly ionized by EUV photons around individual sources overlap. Owing both to the lower photoionization cross sections of H I and He II and to the reduced intensity of the radiation field at X-ray, relative to EUV energies, X-rays alone generally do not produce a fully ionized IGM. However, the primary and secondary ionizations created by X-rays (Shull & van Steenberg 1985, hereafter SVS85) can produce a mild increase in temperature and partial reionization.

A number of authors have examined the reheating of the IGM in association with or preceding reionization itself (Gnedin & Ostriker 1997; Valageas & Silk 1999; Shapiro, Giroux, & Babul 1994; Giroux & Shapiro 1996), while others have studied the effects of X-rays on the high-z IGM

---

[1] Now at Department of Physics and Astronomy, East Tennessee State University.

(Subrahmanyan & Cowsik 1989; Collin-Souffrin 1991; Madau & Efstathiou 1999; Haiman, Abel, & Rees 2000; Oh 2001). The new points of interest presented in this work include self-consistent solutions for the IGM temperature and ionization resulting purely from an XRB, the significant effects of secondary electrons, and the use of more accurate calculations of photoionization cross sections and recombination rate coefficients. We find that the pre-reionization universe may be described by a model in which the first luminous sources and their individual EUV Strömgren spheres are embedded in a preheated, partially ionized IGM, rather than in a cold, completely neutral IGM. However, an early XRB does not create significant amounts of new molecular hydrogen in the IGM, despite the increased population of free electrons. This is primarily due to the strong photodestruction of H^- and H_2 by the near-IR/optical (hereafter IR/O) and the far-UV (UV photons in the Lyman-Werner bands, hereafter FUV) backgrounds, in the respective energy ranges 0.755–11.2 eV and 11.2–13.6 eV, associated with any XRB generated by QSOs. We also find that the enhanced electron fraction in the IGM arising from an XRB prior to reionization may cause an over-estimation of the reionization epoch as determined from the cosmic microwave background (CMB).

The plan of this paper is as follows. In § 2 we outline the IGM heating and cooling processes that we consider and the models for high-z XRBs. In § 3 we present our results and discuss their implications for the cosmological Jeans mass, the CMB, the H^- catalysis of molecular hydrogen, and the inhibition of galactic outflows. We summarize our results in § 4.

2. X-RAY PHOTOIONIZATION MODEL

In this section we detail our assumptions for the XRB and ionizing QSO spectra, and we describe the various processes used to determine self-consistent IGM temperatures and ionization fractions of hydrogen and helium. We focus on the heating and ionizing effects of the X-rays on the initially neutral background IGM, but we do not explicitly follow the growth of individual fully ionized regions around the first QSOs or star-forming galaxies. As reionization begins, the volume filling factor of such highly ionized regions is small. The remaining IGM is cold and neutral, with only a small residual electron fraction ($\sim 10^{-4}$) from the recombination epoch (Seager, Sasselov, & Scott 2000). Highly energetic photons emitted by these sources will propagate much more quickly than their associated ionization fronts. This implies that an epoch will exist when the thermodynamic properties of most of the IGM may be determined by these X-rays.

We model the properties of this volume by solving for ionization and thermal evolution in a uniform primordial medium. We consider the following processes for ionization solutions: photoionization, collisional ionization, case B radiative recombination, dielectronic recombination for He I, and the coupling between H and He caused by the radiation fields from the He I 24.6 eV recombination continuum and from the bound-bound transitions of He I (photon energies at 19.8 and 21.2 eV and the two-photon continuum with an energy sum of 20.6 eV). The last of these processes is incorporated following the method in Osterbrock (1989). The exact form of the photoionization cross sections for H I and He II is taken from Spitzer (1978); we use the fit from Verner et al. (1996) for He I.

We also account for the effects of the secondary ionizations and excitations of H I and He I due to the energetic photoelectrons liberated by the X-rays (SVS85). These introduce a further coupling between the ionization equilibria of H and He. Secondary ionization dominates over direct photoionization for H I in the specialized circumstance where X-rays are the sole source of photoionization. A typical X-ray photon is far more likely to be absorbed by He I rather than H I. The ejected photoelectron, however, will ionize many more H I atoms than He I, as H I is more abundant. As a result, secondary ionizations from He I photoelectrons and the radiation associated with He I recombination and excitation are the primary sources of H I ionization. As pointed out by SVS85, the partitioning of a primary electron's energy, between heating the gas and secondary ionizations and excitations of H I and He I, is itself a function of the gas ionization fraction, x. As x decreases, and in particular for $x \lesssim 0.1$, the photoelectron deposits more of its energy in collisional ionizations/excitations and less in heat. This x-dependence is therefore important to track in the pre-reionization IGM, so that the role of secondary ionizations for H I is not underestimated. In order to be consistent with SVS85, who assumed that the ionization fractions of hydrogen and once-ionized helium were equal, appropriate for the interstellar environment they were considering, we have recast the dependence in their results on x_{H^+} to a direct dependence on the electron fraction, $x_e = n_e/(n_H + n_{He})$, where the number density of electrons $n_e = n_{He\,II} + n_{He\,II} + 2n_{He\,III}$.

We compute the thermal evolution of the IGM including the following processes: photoelectric heating from the secondary electrons of H and He, as prescribed by SVS85 (the SVS85 solution generates less heating relative to a prescription where 100% of the photoelectron's excess energy goes into heating the IGM); and heating from the H I photoelectrons liberated by the bound-bound transitions or the 24.6 eV recombination continuum of He I (here the loss of excess energy to heat is taken to be 100% as further ionizations of H I or He I are not possible). Cooling terms include radiative and dielectronic recombination, thermal bremsstrahlung, Compton scattering off the CMB, collisional ionization and excitation, and the adiabatic expansion of the IGM. The values of the recombination and cooling coefficients for temperatures $\lesssim 10^4$ K were taken from Hummer (1994) and Hummer & Storey (1998), and the heating contribution from the He I two-photon process was calculated using the photon frequency distribution given in Drake, Victor, & Dalgarno (1969). For the purposes of comparison, we will also consider cases that do not include adiabatic cooling, which is mimicked by artificially holding the IGM density constant at its value at $z = 10$, so that there is no expansion cooling for $z < 10$. This would correspond to regions of the IGM that have ceased to participate in the Hubble expansion but have not yet begun to collapse.

The magnitude and spectral shape of the XRB at high redshift are unknown, and a completely self-consistent model of its formation and evolution is beyond the scope of this paper. Although we suggest motivations for our extrapolations of an XRB to early epochs, the three cases below merely provide a theoretical framework in which to study the effects of an XRB at high redshifts. We adopt two basic forms for the high-z XRB, one that is more directly tied to early QSOs, and the other a modified version of the XRB given in Madau & Efstathiou (1999). In the first case,

the specific intensity of each QSO is taken to have a broken power-law form, $I_\nu \propto \nu^{-\alpha}$, where $\alpha = 1.8$ for $h\nu = 13.6$–300 eV (Zheng et al. 1997) and $\alpha = 0.8$ for $h\nu = 300$ eV–10 keV (Washburn et al. 2001). We assume that only those photons with energies $\gtrsim 1$ keV permeate the IGM uniformly, while the less energetic photons are absorbed in the individual host halos. Each QSO's spectrum is further attenuated by absorption by hydrogen or helium in the IGM. If we take the comoving number density of QSOs to have a peak abundance of $\Phi_{QSO} = 10^{-6}$ Mpc^{-3} at $z = 3$ and $f_{QSO} \Phi_{QSO}$ at earlier epochs, then the mean physical (not comoving) separation between QSOs at a given z is

$$d_{QSO} = (100 \text{ Mpc}) f_{QSO}^{-1/3} (1 + z)^{-1} .　(1)$$

We assume then that the cumulative specific intensity in the IGM evolves as d_{QSO}^2, with the evolution of the source density already factored in through f_{QSO}. We normalize the unattenuated mean intensity I_ν such that an extrapolation down to 13.6 eV, using the QSO's intrinsic spectral shape, is $I_0 = 10^{-21}$ ergs cm^{-2} s^{-1} Hz^{-1} sr^{-1} at $z = 3$, consistent with observational constraints (see, e.g., Haardt & Madau 1996; Fardal, Giroux, & Shull 1998 and references therein). Realistically, this underestimates the corresponding X-ray contribution because the radiation at 13.6 eV is subject to some attenuation from the IGM, even at $z = 3$.

Combining the above factors, we may parameterize the evolution of the IGM-filtered specific intensity for $z \geq 3$ as

$$I_\nu = 3.8 \times 10^{-24} \left(\frac{h\nu}{300 \text{ eV}} \right)^{-0.8} f_{QSO}^{2/3} e^{-\tau_\nu}$$

$$\times \left(\frac{1 + z}{4} \right)^2 \text{ ergs cm}^{-2} \text{ s}^{-1} \text{ Hz}^{-1} \text{ sr}^{-1} ,　(2)$$

where we adopt $f_{QSO} = 10^{-0.5(z-3)}$ from the SDSS collaboration (Fan et al. 2001a), and $\tau_\nu = d_{QSO}[n_{H^0} \sigma_\nu(H^0) + n_{He^0} \sigma_\nu(He^0) + n_{He^+} \sigma_\nu(He^+)]$ is the IGM optical depth, with σ_ν being the appropriate photoionization cross section for each species. Henceforth, we refer to the above XRB as case S (for the Sloan survey).

An alternate prescription for the high-z XRB is given in Madau & Efstathiou (1999), in which the present-day XRB evolves as $(1 + z)^3$, weighted by an exponential cutoff factor to account for the decreasing source density at high redshift. The specific intensity of this XRB is given by equation (6) of Madau & Efstathiou (1999) in units of keV cm^{-2} s^{-1} keV^{-1} sr^{-1}, which, over the energy range 1–10 keV, we take to be

$$I_\nu = 7.7 \left(\frac{h\nu}{1 \text{ keV}} \right)^{-0.29} \exp\left(-\frac{h\nu}{40 \text{ keV}} \right)$$

$$\times (1 + z)^3 \exp\left[-\left(\frac{z}{z_c} \right)^2 \right] .　(3)$$

We will consider two cases of this XRB: case 1 with $z_c = 5$, as in Madau & Efstathiou (1999), and case 2 without the exponential cutoff factor, as in Collin-Souffrin (1991) where the XRB evolves cosmologically as a radiation field. The assumed specific intensity of each XRB increases from case S through cases 1 and 2. At $z = 9$, for example, their respective values at 2 keV are 4.4×10^{-26}, 1.6×10^{-24}, and 4×10^{-23} ergs cm^{-2} s^{-1} Hz^{-1} sr^{-1}.

The evolution of the temperature and ionization fractions is calculated as follows. We take the background cosmology

to be described by $\Omega_m = 0.3$, $\Omega_\Lambda = 0.7$, $h = 0.7$, $\Omega_b h^2 = 0.019$, $T_{CMB,0} = 2.728$ K, and $Y_{He} = 0.24$. The calculation is begun at $z = 12$, with an initial IGM temperature of 20 K and residual ionization fractions of $x_{H^+} = 10^{-4}$ and $x_{He^+} = 10^{-9}$. We consider XRBs in the redshift range $7 < z < 12$; the lower limit is roughly the latest epoch from observational limits (Fan et al. 2001b; Becker et al. 2001) that can be considered as being prior to reionization, while at $z = 12$ horizon effects begin to attenuate the XRB. We demonstrate the latter by equating the light crossing time for half the mean physical source separation (given by eq. [1]) with the age of the universe for XRB case S, accounting for the finite time needed for the X-ray photons from individual sources to permeate the IGM. As case S is the weakest XRB considered here, with the lowest source density, this yields a conservative lower limit to the redshift at which horizon effects become important. Furthermore, the Eddington accretion timescale is $\sim 4.5 \times 10^7$ yr, assuming an average QSO radiative efficiency of 10%. Since this corresponds to $z \sim 50$ in our adopted cosmology, by $z = 12$, sources have had $\sim 4 \times 10^8$ yr (many times their Eddington timescale) to form and generate an XRB (see, however, Haiman & Loeb 2001 on how this may not prove sufficient for the formation of the most massive black holes that likely power the brightest QSOs).

Our numerical solution for the evolving thermodynamic properties of the IGM solves the nonequilibrium rate equations and energy equation for the expanding IGM (see Giroux & Shapiro 1996, eqs. [2.1]–[2.4]). We do not follow the nonequilibrium formation and destruction of H_2, and we do not consider detailed radiative transfer. The equations are integrated with a fourth-order Runge-Kutta scheme with the time steps set to be less than 3% of the shortest relevant thermal or ionization timescale.

3. RESULTS AND IMPLICATIONS

In Figures 1–3 we show the temperature and hydrogen and helium ionization fractions of the IGM as a function of redshift for XRB cases 1 and 2. Case S was found to have negligible effects on the thermal and ionization properties of the IGM and did not alter them appreciably, over the redshifts that we consider, from their values in an expanding
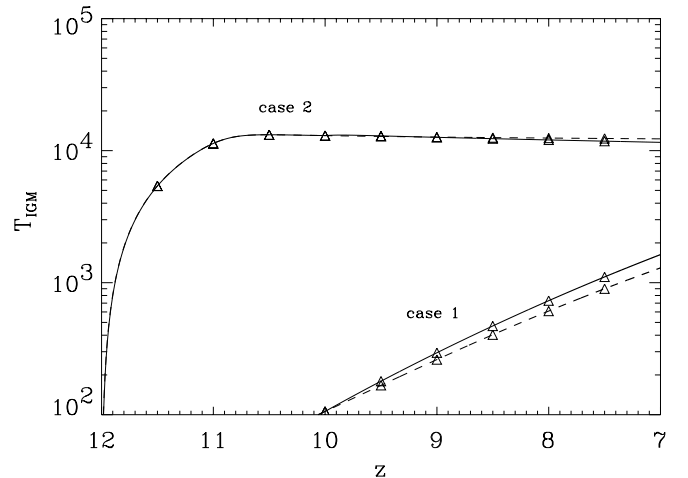

FIG. 1.—IGM temperature shown as a function of redshift for the two XRBs described in the text, each with (*dashed lines*) and without (*solid lines*) adiabatic cooling from cosmological expansion.
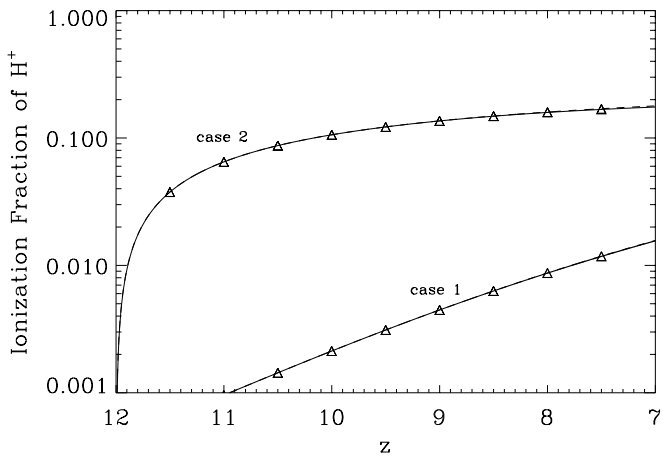
FIG. 2.—IGM ionization fraction of hydrogen shown as a function of redshift for the two XRBs described in the text, each with (*dashed lines*) and without (*solid lines*) adiabatic cooling from cosmological expansion.

IGM without any X-rays. We therefore do not include case S in the figures but emphasize that our first result is that there will be no significant effects on the evolving IGM for a conservative estimate of the pre-reionization XRB.

The plots show that, depending on the choice of the XRB, the IGM temperature ranges from ~ 100 to $\sim 10^4$ K, with x_{H^+} varying from 0.1% to $\sim 20\%$. For each case, the solutions including and excluding adiabatic cooling are almost identical and are practically overlaid in the figures. As may be expected, the stronger the XRB, the greater are the heating and ionization of the IGM. Although we do not show it here, an XRB whose magnitude lies between those of cases 1 and 2 generates IGM temperatures and ionization fractions that are bracketed by the two cases shown in the figures.

Note that for case 2, T_{IGM} is slightly higher when adiabatic cooling is included rather than excluded. This counterintuitive result arises from our choice to mimic the cases without adiabatic cooling by stopping the cosmological evolution of the IGM density at $z = 10$. For case 2, by $z = 10$, cooling is dominated by line excitation cooling, which is proportional to the square of the IGM density, and
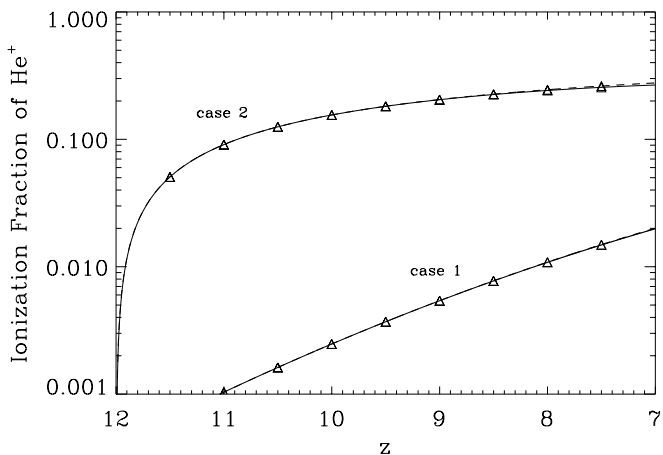

FIG. 3.—IGM ionization fraction of He$^+$ shown as a function of redshift for the two XRBs described in the text, each with (*dashed lines*) and without (*solid lines*) adiabatic cooling from cosmological expansion.

not adiabatic cooling. Consequently, for the cases including adiabatic cooling, where the IGM density continues to decrease at $z < 10$, the cooling decreases more rapidly than it does in the absence of adiabatic cooling, leading to marginally larger values of T_{IGM}. Note also that when x_e, which roughly tracks x_{H^+}, exceeds about 10% (case 2), secondary ionization becomes less important for H I, and x_{He^+} begins to exceed x_{H^+}. We find that the He III fraction $x_{He^{+2}}$ was typically smaller by a factor of 100 than x_{He^+}, and we do not display it in the figures.

We note here some consequences of our adopted photoionization cross sections and of consistently including the secondary effects of photoelectrons. The He I cross section is taken from the fit to experimental data provided by Verner et al. (1996). This differs dramatically in the keV energy range from the two–power-law fit from Osterbrock (1989) used by Shapiro & Kang (1987) and Abel et al. (1997), which is only valid for photon energies of a factor of a few above the threshold value of 24.6 eV. This power-law extrapolation exceeds the Verner et al. (1996) He I cross section by a factor of 40 at 1 keV and by a factor of 400 at 10 keV. It is therefore important to use the latter fit for He I when considering the effects of a pure XRB. Furthermore, the ratio of the H I/He I photoionization cross sections is very small in the X-ray range, about 3% for photon energies of 1–10 keV. Thus, in the pre-reionization universe, when the IGM is predominantly neutral and can be permeated only by X-rays, the ionization balance is driven primarily by the photoionization of He I and its associated photoelectrons (and not those from H I), each of which then ionizes about a dozen hydrogen atoms (SVS85). Since the primordial ratio of helium to hydrogen is about 8%, we may anticipate that $x_{He^+} \sim x_{H^+}$ in such a scenario, and that is what we find.

For the purposes of the discussion below, we now take case 2 with adiabatic cooling to be our fiducial case, as it provides an upper bound to the magnitude of the results in Figures 1–3, or equivalently, it represents the "maximal effect" of a high-z XRB. In this case, H I ionization is dominated by secondary ionizations from the He I photoelectrons, as expected, followed by radiation from the bound-bound transitions of He I, while He I is most affected by direct photoionization and secondary ionizations from its own photoelectrons. The major sources of IGM heating are, in decreasing order, direct photoelectric heating of He I, H I, and He II and heating from the bound-bound transitions of He I. At the earliest epochs that we consider, adiabatic expansion and Compton cooling were the dominant cooling processes. For case 2, by $z \sim 11$, the IGM had experienced sufficient heating and ionization that line excitation cooling was the most significant source of cooling. For case 1, adiabatic expansion remained the dominant cooling term.

3.1. Jeans Mass Filtering

We now discuss the implications of such a heated, partially ionized IGM, beginning with the evolution of overdensities in a warm IGM. At any redshift, dark matter perturbations with virial temperatures $T_{vir}(z)$ will decouple from universal expansion on the associated mass scales and begin to collapse. The baryons will also fall into these dark matter potential wells if they have little pressure associated with them. If the gas in the IGM is heated by luminous sources, and if T_{IGM} exceeds T_{vir}, the baryons will resist col-

lapse on the mass scale set by T_{IGM}, leading to a filtering of the mass scale that can collapse and virialize. This feedback from a heated IGM has been explored for a number of reheating scenarios (Tegmark et al. 1997; Shapiro et al. 1994; Valageas & Silk 1999). As we do not account for gas clumping in our analysis, we follow Shapiro et al. (1994) in evaluating the magnitude of the filtering for the cosmological Jeans mass. Assuming that the temperature of the baryons and the CMB are coupled until $z \sim 150$ and that the IGM cools adiabatically after that, the Jeans mass in baryons is

$$M_J \approx 2.2 \times 10^3 \left[\frac{\Omega_b}{h(\mu\Omega_m)^{1.5}} \right] \left(\frac{1+z}{10} \right)^{1.5} M_\odot . \quad (4)$$

If, however, the IGM is heated to a temperature T_{IGM}, the Jeans mass will scale as

$$M_J \approx 1.3 \times 10^5 \left[\frac{\Omega_b}{h(\mu\Omega_m)^{1.5}} \right] \left(\frac{T_{IGM}}{T_{CMB}} \right)^{1.5} M_\odot , \quad (5)$$

where $T_{CMB} = T_{CMB,0}(1+z)$. For the purposes of comparison, we work with the fiducial case defined above. At $z = 9$, $T_{IGM} \sim 1.3 \times 10^4$ K, so that $M_J \sim 3 \times 10^8 M_\odot$, as opposed to $M_J \sim 520 M_\odot$ from equation (4). Thus, the Jeans mass in a preheated IGM exceeds by several orders of magnitude its corresponding value in the case of an IGM that cools adiabatically after decoupling from the CMB. Furthermore, the filtered Jeans mass increases with decreasing z, unlike the canonical Jeans mass.

3.2. The CMB

A partially ionized IGM can affect the CMB through Thomson scattering of the CMB photons off the free electrons in the IGM. There are at least two potentially observable effects. First, the optical depth to electron scattering, τ_e, as measured from the primary CMB anisotropies, will have some contribution from the partially ionized IGM preceding complete reionization and may no longer be a strong constraint on the epoch of reionization. The expression for τ_e as a function of redshift in a Λ cosmology is given by (see, e.g., Tegmark & Silk 1995)

$$\tau_e(z) \simeq 0.057\Omega_b h \int_0^z dz' \frac{(1+z')^2 x_e(z')}{\sqrt{\Omega_\Lambda + (1+z')^2(1 - \Omega_\Lambda + \Omega_m z')}} . \quad (6)$$

This assumes that all the baryons are in a homogeneous IGM at all times, which may not be a fair approximation at late epochs. As a simple calculation, let us examine two possibilities. First, we assume that reionization occurred at $z = 6$ and that x_{H+} is given by our standard XRB for $7 \leq z \leq 12$, with a post-recombination residual ionization fraction of 10^{-4} for $12 < z < 1000$. The values of x_{H+} are linearly extrapolated between redshifts of 6 and 7. The second case assumes that there is no high-z XRB and that $x_{H+} = 10^{-4}$ for $7 \leq z \leq 1000$. Figure 4 displays τ_e as a function of redshift for these two scenarios. In the former case, the integrated optical depth to recombination is $\tau_e \sim 0.047$, of which 0.032, or about 68%, is from the reionized IGM, and 0.009 comes from the partially ionized IGM, roughly a 20% effect. Although this seems to be a small correction, it is a level of accuracy that can in principle be probed by future CMB experiments such as *Planck* (Eisenstein, Hu, &
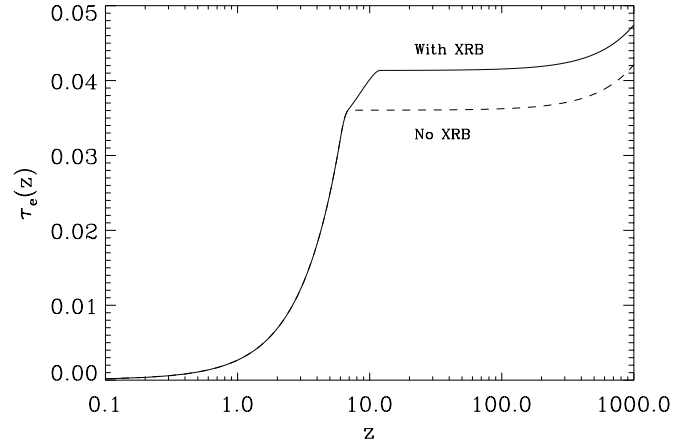
FIG. 4.—Optical depth to electron scattering as a function of redshift. Solid line assumes reionization of the IGM at $z = 6$, partial ionization for $7 \leq z \leq 12$ for XRB case 2 with adiabatic cooling, and the primordial electron freeze-in abundance at higher redshifts. Dashed line represents the same scenario, but with no XRB.

Tegmark 1999). The additional contribution from the partially ionized IGM could cause an overestimation of the reionization epoch, z_r, if the cumulative optical depth were attributed solely to the IGM after complete reionization. Unfortunately, the correction to τ_e from this XRB has roughly the same value as that from the IGM's residual electron fraction at $12 < z < 1000$ ($\tau_e \sim 0.006$), as a result of the late reionization model and a low total τ_e.

Since the theoretical uncertainty in the post-recombination x_e is of order 10% at present, all that is required to distinguish between the "with XRB" case in Figures 4 and 5 and a "no XRB" case with somewhat earlier full reionization is an independent measurement of z_r. While *Planck* could in principle map out the low-multipole (l) polarization peak caused by reionization in the CMB angular power spectrum to significant accuracy, for late reionization this feature is of sufficiently low magnitude and at large enough scales ($l \lesssim 10$) that foregrounds are likely to be a complication. Ultimately, a spectroscopic determination of the reionization epoch via the Gunn-
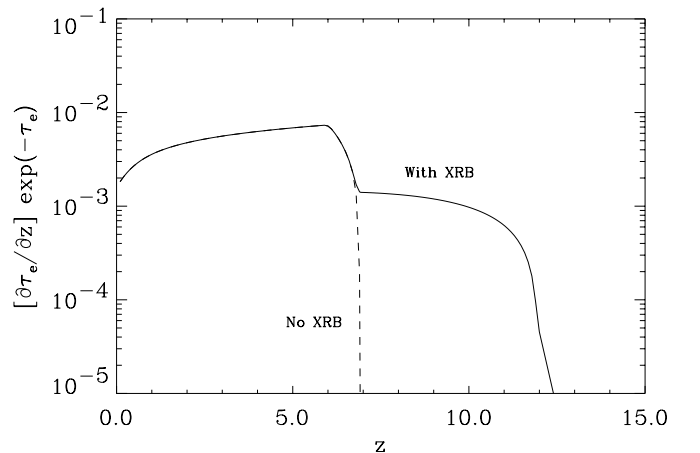
FIG. 5.—Probability distribution of a CMB photon being Thomson scattered by an IGM electron as a function of redshift, with the same assumptions as in Fig. 4.

Peterson effect from the SDSS or from the *Next Generation Space Telescope*, in conjunction with future CMB data, may provide the best probe of an IGM partially ionized by X-rays prior to full reionization. The first of these observations is a real possibility in the near future from efforts that are well underway with data on SDSS QSOs at redshifts $\gtrsim 5.8$ (Fan et al. 2001b; Becker et al. 2001). Otherwise, for all practical purposes, it may be a challenge to separate these two different contributions to τ_e from the epochs preceding reionization.

Although a partially ionized IGM may smear a direct relation between τ_e and z_r as determined from the CMB, the majority of CMB photons that are Thomson scattered at late times are still scattered by a fully ionized IGM. To see this, consider that the probability that a CMB photon scattered off an IGM electron after redshift z along the line of sight is $1 - \exp\left[-\tau_e(z)\right]$. The derivative of this, called the visibility function (see, e.g., Tegmark et al. 1994), is the relative probability of the last scattering redshift of a CMB photon. We show the visibility function in Figure 5, for the two scenarios in Figure 4. We see that, despite the contribution to τ_e from an IGM that is partially ionized by X-rays, the surface of last scattering after recombination for the CMB photons that we see today is still strongly biased toward the epochs following complete reionization. Although we do not display it here, we note that the peak in the visibility function corresponding to recombination is much larger than that associated with reionization (see, e.g., Zaldarriaga 1997), especially when the latter occurs at low redshifts.

A second signature involves the correlations between ionized regions in a patchy reionization model, which appear in the multipole moments of the CMB anisotropies, typically at very small angular scales ($l \gtrsim 5000$; Knox, Scoccimarro, & Dodelson 1998). Since these correlations are usually predicted assuming a neutral background IGM, one may pose the question of whether such correlations may be significantly erased in the presence of a partially ionized IGM. As it happens, this is not a concern since the dominant contribution to the above correlations comes from patches of full ionization, which are themselves highly correlated with high-density regions. Thus, the relevant factor is the correlation of the underlying matter density field, rather than the sizes of ionized ($x = 1$) regions or the ionization contrast between $x = 1$ regions and the background IGM. The relative contributions from these different effects is best seen in Valageas, Balbi, & Silk (2001).

3.3. *Molecular Hydrogen*

We now turn to the implications of an X-ray–heated, partially ionized IGM for the production of molecular hydrogen, H_2, which is an important coolant for primordial gas in virializing structures. A prerequisite for this is that the baryons are able to collapse into virializing dark matter halos, which may be hindered by a heated IGM, as discussed above. We emphasize that we focus here on H_2 creation and destruction in the IGM, rather than within dense collapsed structures. We include the following processes in an equilibrium calculation of the abundance of H_2 relative to hydrogen, in which we consider only the H^- creation channel and do not include formation via H_2^+ (Lepp & Shull 1984; Abel et al. 1997). Unless stated otherwise, rates for individual reactions are taken from Donahue & Shull (1991). H^- is formed through radiative attachment of H I

(Galli & Palla 1998) and is destroyed by associative detachment by H I, mutual neutralization with protons, collisional detachment by electrons (Abel et al. 1997), and photodetachment by photons of energy 0.755–13.6 eV. We assume that H_2 forms by associative detachment of H I and H^- and is destroyed by collisions with electrons and with H I, by charge exchange with protons, and by photodissociation in the Lyman and Werner bands by photons of energies 11.2–13.6 eV.

As we do not specifically account for radiation below ~ 1 keV, we extrapolate the flux of each XRB at 2 keV down to 2500 Å (4.97 eV) using an effective X-ray spectral index of $\langle \alpha_{0,X} \rangle = -1.38$, with a $v^{-0.5}$ power law for photon energies below about 5 eV. We then compute the photodissociation rate of H^- directly from the tabulated cross sections of Wishart (1979), using the fit given in Tegmark et al. (1997), and of H_2 as described in Donahue & Shull (1991), for the respective photon energy ranges stated above. For both H^- and H_2, particularly the latter, the photodissociation rates exceed the other destruction channels by several orders of magnitude. As we have performed an equilibrium calculation and have not included the post-recombination freeze-in abundance of H_2 relative to hydrogen of $\sim 10^{-6}$ in the IGM, our results should be taken as representing the effect of an XRB for newly created or destroyed H_2.

We find that, for XRB cases 1 and 2, $n(H_2)/n_H$ never exceeds about 3×10^{-14} and has little evolution over the redshifts that we consider; this falls well short of the critical value of $\sim 10^{-6}$ to stimulate gas cooling in high-z structures. Although the presence of X-rays boosts the free electron fraction, at any given redshift the stronger XRB creates less new H_2, owing to the combination of various dissociation processes that are enhanced in a heated IGM and to the strong role played by photodissociation in the destruction of both H^- and H_2. We find that the timescales associated with the formation and photodestruction of H^- and H_2 are always much less than the Hubble time at each epoch, so that our equilibrium calculations here indicate real changes to the primordial freeze-in abundance of H_2.

To illustrate the relative roles played by an XRB and the associated radiation fields below 13.6 eV, we display in Table 1 the equilibrium abundances of H^- and H_2 calculated by successively including radiation from two backgrounds, defined as follows. The FUV includes the photons relevant for H_2 photodissociation in the Lyman-Werner bands (11.2–13.6 eV). The H^- is dissociated by photons having energies of 0.755–13.6 eV, in the framework of this paper. For the purposes of Table 1, however, the IR/O (infrared/optical) term refers to the inclusion of all sub–13.6

TABLE 1
MOLECULAR HYDROGEN PRODUCTION

Background	$n(H^-)/n_H$	$n(H_2)/n_H$
XRB	1.1×10^{-7}	1.6×10^{-5}
XRB+IR/O	3.3×10^{-12}	4.8×10^{-10}
XRB+FUV	1.1×10^{-7}	4.2×10^{-10}
XRB+FUV+IR/O	3.3×10^{-12}	1.2×10^{-14}

NOTE.—The relative roles played by X-ray, FUV (Lyman-Werner bands), and IR/optical backgrounds (see text for the individual definitions of photon energy ranges) in an equilibrium calculation of $n(H^-)$ and $n(H_2)$ for XRB case 2 with adiabatic cooling at $z = 9$.

eV photons except those in the Lyman-Werner bands. Although this energy range (0.755–11.2 eV) corresponds to some UV photons as well, most of the photodissociation occurs at near-IR and optical wavelengths, given the nature of the H^- cross section and our adopted power-law form for the background intensity at these energies.

We see that the minimum IR/O and FUV backgrounds associated with any putative XRB from high-z quasars more than compensate for any positive feedback from the XRB in the form of an increased electron fraction in the IGM (see, however, Ricotti, Gnedin, & Shull 2001 on the positive feedback for H_2 formation in the vicinity of individual ionization fronts generated by hard stellar spectra). The negative feedback from FUV radiation has already been noted in several works; we point out here the additional feedback from IR/O photons. The importance of the IR/O photons in this paper relative to the results of previous works (e.g., Haiman et al. 2000) can be traced to at least two factors. Firstly, our equilibrium calculation is performed for the relatively low density conditions in the IGM at $z = 9$, rather than within highly overdense collapsed halos, so that some variance can be attributed to the differing densities of the studied environments. Secondly, Table 1 represents the effects of the strongest XRB considered here, which has a correspondingly high IR/O associated background. An XRB that was extrapolated from the observed EUV specific intensity at $z = 3$, such as case S in this work, would have a related IR/O background that has a negligible impact on the net H^-, and hence H_2, abundances. Note also that a combination of these two factors, IGM density and radiation intensity at the H^- photodissociation threshold, implies that only a relatively modest IR/O background is required at $z < 12$ to destroy H^-. A radiation field of far greater energy density is needed to accomplish this in the early universe; this leads to the well-known result that the CMB photons are believed to have photodissociated H^- at $z \gtrsim 100$.

Our estimate of the FUV background is not necessarily the minimal value, as a result of the opacity of the IGM in the Lyman-Werner bands, which we have not accounted for here. The table shows, however, that even an order of magnitude reduction in the FUV background alone will not increase the fractional abundance of H_2 above 10^{-6}. As we have neglected contributions from stellar radiation, we have in fact underestimated the effects of IR/O and FUV photons at the epochs we consider. In summary, we find that an XRB does not produce significant amounts of new H_2 in the IGM, unless the associated FUV and IR/O backgrounds were somehow strongly attenuated.

3.4. *Inhibition of Outflows*

Finally, it may be possible for a heated IGM with sufficient pressure to inhibit outflows from star-forming protogalaxies. Mass loss from early objects through galactic winds or evaporation is often invoked to explain the ubiquitous presence of metals in the Lyα forest clouds at $z \sim 3$; a preheated IGM could, however, hinder such outflows of metal-enriched gas from host galaxies at sufficiently high redshifts (prior to reionization). An estimate of the effect of a warm IGM in inhibiting galactic winds may be made as follows. Setting the ram pressure of the wind, $\rho_w v_w^2$, equal to $P_{IGM} = (n_H + n_{He} + n_e)kT_{IGM}$, and using $\dot{M}_w = 4\pi r_{st}^2 \rho_w v_w$, where $\dot{M}_w$ and r_{st} are, respectively, the mass outflow rate of the wind and the wind stalling radius in the IGM where

pressure equilibrium is reached, we have

$$r_{st} \simeq (0.5 \text{ Mpc})$$
$$\times \left[\left(\frac{\dot{M}_w}{M_\odot \text{ yr}^{-1}} \right) \left(\frac{v_w}{10^3 \text{ km s}^{-1}} \right) \left(\frac{10^4 \text{ K}}{T_{IGM}} \right) \left(\frac{10}{1+z} \right)^3 \right]^{1/2} \quad (7)$$

for the IGM density at $z = 9$. Note that if the IGM had cooled adiabatically from $z \sim 150$, then T_{IGM} would be a few kelvin, and $r_{st} \sim 33$ Mpc. This neglects the added contribution that any ionizing photons escaping from the protogalaxy would make to the local ambient pressure.

Equation (7) approximately indicates the maximum degree, case 2 being the strongest XRB considered here, to which an early XRB may hinder outflows from star-forming galaxies at $z = 9$. Note, however, that at lower redshifts, e.g., $z \sim 3$, r_{st} can be significantly larger, particularly for the mass outflow rates of a few to 10 $M_\odot$ yr^{-1} that are typical of starbursting galaxies. Thus, the observation of a trace metallicity in the IGM at $z \sim 3$ does not necessarily rule out an early XRB from QSOs prior to reionization, if the epoch of metal ejection associated with stellar activity in high-z galaxies succeeds that of preheating from an XRB by a sufficiently long period. This becomes a particularly important constraint, however, for a model that posits an early XRB from stars, or one that explores the heating effects of X-rays for the post-reionization IGM (Madau & Efstathiou 1999).

4. CONCLUSIONS

We have examined the effects of various high-z XRBs, including a case that mimics X-ray photons from early bright QSOs, on the temperature and ionization of the IGM before reionization is complete. We have found that individual luminous sources with their associated H II/He III ionized regions may be embedded in a warm, partially ionized IGM, rather than in a cold neutral IGM, during the epochs before individual Strömgren spheres have overlapped.

The heating and ionizing effects from the XRBs were determined self-consistently, including the associated generation of photoelectrons that act as secondary sources, resulting in an enhanced population of free electrons. We have investigated two XRB cases that are related to the measured present-day soft XRB and find that they can heat the IGM to temperatures between 100 and 10^4 K prior to reionization and result in ionization levels between fractions of a percent to about 20%. The third XRB, assumed to be generated by early QSOs whose space density evolves as indicated by the recent observations of bright high-z quasars from the SDSS collaboration, did not appreciably alter the IGM temperature and ionization from their post-recombination values at the redshifts we considered.

We have examined the implications of our results for several phenomena of interest to cosmology, including the Jeans mass, the CMB, and the production of H_2. In particular, the preheated IGM raises the Jeans mass significantly at the redshifts of interest to the growth of structure, leading to a filtering of the baryonic mass scales that can collapse into virializing dark matter halos. We also find that the XRB-enhanced electron fraction in the IGM prior to reionization increases the total optical depth to electron scattering. This could lead to an overestimation of the reionization epoch if the cumulative τ_e as measured by CMB experiments were attributed solely to the fully ionized IGM. However, the

addition to τ_e from the post-recombination IGM, with a freeze-in $x_e \sim 10^{-4}$ for $z \lesssim 1000$, is roughly comparable to that from an IGM that is partially ionized by our standard XRB. It may be a challenge to observationally distinguish these disparate contributions to τ_e in late reionization scenarios, unless there is an independent measurement of the reionization epoch, e.g., spectroscopically through the Gunn-Peterson effect from the SDSS or from future space telescopes. Such a constraint seems particularly promising from ongoing analyses that are well underway with SDSS data on QSOs at $z \gtrsim 5.8$ (Fan et al. 2001b; Becker et al. 2001). In conjunction with forthcoming CMB data, it could provide the best probe of an IGM partially ionized by X-rays prior to full reionization, which otherwise may not leave a unique imprint in the CMB. Finally, if the IGM is heated prior to reionization, its thermal pressure could suppress outflows from galaxies. A preheated IGM may also be detected by future radio telescopes in 21 cm emission against the CMB (Tozzi et al. 2000).

Despite the increased electron fraction in the IGM, the amount of H^--catalyzed molecular hydrogen formed is insignificant, contrary to expectations. This is primarily due to the strong photodissociating effects of the minimum IR/O and FUV (Lyman-Werner bands) backgrounds associated with any high-z XRB on H^- and H_2, respectively. As we have neglected radiation from stars in the treatment here, we have underestimated these photo-destruction terms at the redshifts we consider. We therefore conclude that, unless the FUV and IR/O backgrounds are strongly attenuated by some process that we have not included here (see Table 1), the positive feedback from a boosted electron fraction caused by a high-z XRB is not sufficient to produce interesting amounts of new H_2 in a uniform IGM.

We mention here that there are several issues that we have neglected or oversimplified in this paper. First, we have not included the effects of any clumping in the IGM, which will reduce our adiabatic cooling estimates, alter the equilibrium calculation values of $n(H_2)$, and challenge our assumption that the X-rays heat the IGM homogeneously. Second, although we have noted the Jeans mass filtering in a heated IGM, we have not examined in detail the further cooling that must occur in virializing halos in order for star formation to occur. We have found that an XRB may not create significant amounts of new H_2 in the IGM, but the situation may prove to be different within a halo or an IGM overdensity that is being irradiated by X-rays from a nearby source (see, e.g., Ricotti et al. 2001). In such cases, the favored regimes of baryon density and temperature for H_2 production may change. It would be interesting to explore the feedback of a heated partially ionized IGM on nonequilibrium H_2 chemistry in the presence of a (destroying) FUV versus (enhancing) XRB photon field (Haiman et al. 2000), particularly when including the effects of secondary electrons in a dense, neutral halo at high redshift. We defer more detailed treatments of these problems and related consequences to future work.

REFERENCES

Abel, T., Anninos, P., Zhang, Y., & Norman, M. L. 1997, NewA, 2, 181
Becker, R. H., et al. 2001, AJ, in press
Chiu, W. A., & Ostriker, J. P. 2000, ApJ, 534, 507
Ciardi, B., Ferrara, A., Governato, F., & Jenkins, A. 2000, MNRAS, 314, 611
Collin-Souffrin, S. 1991, A&A, 243, 5
Donahue, M., & Shull, J. M. 1987, ApJ, 323, L13
———. 1991, ApJ, 383, 511
Drake, G. W. F., Victor, G. A., & Dalgarno, A. 1969, Phys. Rev., 180, 25
Eisenstein, D. J., Hu, W., & Tegmark, M. 1999, ApJ, 518, 2
Fan, X., et al. 2000, AJ, 120, 1167
———. 2001a, AJ, 121, 54
———. 2001b, AJ, in press
Fardal, M. A., Giroux, M. L., & Shull, J. M. 1998, AJ, 115, 2206
Fukugita, M., & Kawasaki, M. 1994, MNRAS, 269, 563
Galli, D., & Palla, F. 1998, A&A, 335, 403
Giacconi, R., et al. 2001, ApJ, 551, 624
Gilli, R., Risaliti, G., & Salvati, M. 1999, A&A, 347, 424
Giroux, M. L., & Shapiro, P. R. 1996, ApJS, 102, 191
Gnedin, N. Y. 2000, ApJ, 535, 530
Gnedin, N. Y., & Ostriker, J. P. 1997, ApJ, 486, 581
Haardt, F., & Madau, P. 1996, ApJ, 461, 20
Haiman, Z., Abel, T., & Rees, M. J. 2000, ApJ, 534, 11
Haiman, Z., & Loeb, A. 1997, ApJ, 483, 21
———. 1998, ApJ, 503, 505
———. 2001, ApJ, 552, 459
Hogan, C. J., Anderson, S. F., & Rugers, M. H. 1997, AJ, 113, 1495
Hu, E. M., McMahon, R. G., & Cowie, L. L. 1999, ApJ, 522, L9
Hummer, D. G. 1994, MNRAS, 268, 109
Hummer, D. G., & Storey, P. J. 1998, MNRAS, 297, 1073
Jakobsen, P., Boksenberg, A., Deharveng, J. M., Greenfield, P., Jedrzejewski, R., & Paresce, F. 1994, Nature, 370, 35
Knox, L., Scoccimarro, R., & Dodelson, S. 1998, Phys. Rev. Lett., 81, 2004
Kormendy, J., & Gebhardt, K. 2001, in Proc. of the 20th Texas Symposium on Relativistic Astrophysics, ed. H. Martel & J. C. Wheeler, in press (astro-ph/0105230)
Kriss, G. A., et al. 2001, Science, 293, 1112
Lepp, S., & Shull, J. M. 1984, ApJ, 280, 465
Madau, P., & Efstathiou, G. 1999, ApJ, 517, L9

Madau, P., Haardt, F., & Rees, M. J. 1999, ApJ, 514, 648
Magorrian, J., et al. 1998, AJ, 115, 2285
Mushotzky, R. F., Cowie, L. L., Barger, A. J., & Arnaud, K. A. 2000, Nature, 404, 459
Oh, S. P. 2001, ApJ, 553, 499
Osterbrock, D. E. 1989, Astrophysics of Gaseous Nebulae and Active Galactic Nuclei (Mill Valley: University Science Books)
Reimers, D., Kohler, S., Wisotzki, L., Groote, D., Rodriguez-Pascual, P., & Wamsteker, W. 1997, A&A, 327, 890
Ricotti, M., Gnedin, N. Y., & Shull, J. M. 2001, ApJ, 560, 580
Seager, S., Sasselov, D. D., & Scott, D. 2000, ApJS, 128, 407
Shapiro, P. R., Giroux, M. L., & Babul, A. 1994, ApJ, 427, 25
Shapiro, P. R., & Kang, H. 1987, ApJ, 318, 32
Shaver, P. A., Hook, I. M., Jackson, C. A., Wall, J. V., & Kellermann, K. I. 1999, in ASP Conf. Ser. 156, Highly Redshifted Radio Lines, ed. C. L. Carilli et al. (San Francisco: ASP), 163
Shull, J. M., & van Steenberg, M. E. 1985, ApJ, 298, 268 (SVS85)
Spinrad, H., Stern, D., Bunker, A., Dey, A., Lanzetta, K., Yahil, A., Pascarelle, S., & Fernandez-Soto, A. 1998, AJ, 116, 2617
Spitzer, L. 1978, Physical Processes in the Interstellar Medium (New York: Wiley)
Subrahmanyan, R., & Cowsik, R. 1989, ApJ, 347, 1
Tegmark, M., & Silk, J. 1995, ApJ, 441, 458
Tegmark, M., Silk, J., & Blanchard, A. 1994, ApJ, 420, 484
Tegmark, M., Silk, J., Rees, M. J., Blanchard, A., Abel, T., & Palla, F. 1997, ApJ, 474, 1
Tozzi, P., Madau, P., Meiksin, A., & Rees, M. J. 2000, ApJ, 528, 597
Tumlinson, J., & Shull, J. M. 2000, ApJ, 528, L65
Valageas, P., Balbi, A., & Silk, J. 2001, A&A, 367, 1
Valageas, P., & Silk, J. 1999, A&A, 347, 1
Verner, D. A., Ferland, G. J., Korista, K. T., & Yakovlev, D. G. 1996, ApJ, 465, 487
Washburn, K., Reynolds, C. S., Shull, J. M., & Nowak, M. A. 2001, in preparation
Wishart, A. W. 1979, MNRAS, 187, 59P
Zaldarriaga, M. 1997, Phys. Rev. D, 55, 1822
Zheng, W., Kriss, G. A., Telfer, R. C., Grimes, J. P., & Davidsen, A. F. 1997, ApJ, 475, 469